Mem. S.A.It. Vol. 79, 569

Memorie della

Mixing processes in rotating stars

S. Talon

Département de Physique, Université de Montréal, Montréal PQ H3C 3J7, Canada
e-mail: talon@astro.umontreal.ca

Abstract. In this review, I describe physical mechanisms associated with mixing in rotating stars. These include the well-known meridional circulation and shear instabilities treated in many stellar evolution codes. I also briefly discuss the possible impact of a large scale magnetic field, and describe the role of internal gravity waves for the transport of angular momentum.

Key words. Hydrodynamics – Turbulence – Waves – Methods: numerical – Stars: interiors – Stars: rotation

1. Introduction

The need for extra mixing in stars is now widely recognized, and different rotational histories could well explain the variety of stellar behaviors. While early descriptions of rotational mixing have relied on simple power laws relating the amount of mixing to the star's rotation rate, it was soon recognized that self-consistent models that take into account the angular momentum evolution must be built (Endal & Sofia 1976).

1.1. Shear instability

As solid body rotation correspond to a lowest energy state, differential rotation gives rise to a pleiades of instabilities. Here, we focus on shear, which is the most efficient and thus, the most used in stellar models. For a detailed review of other well studied instabilities, see *e.g.* Talon (2007) and references therein.

The *linear* stability criterion against shear states that there must be no inflection point in the velocity profile for it to be stable (Rayleigh 1880). However, experiments show that turbulence can develop even in the absence of such an inflection point and this is interpreted in terms of *finite amplitude* fluctuations. This non-linear regime may be tackled with the energetics of the problem. To extract energy from differential rotation, one must be able to overcome the density stratification. By comparing kinetic and potential energies and assuming adiabaticity, one obtains the Richardson instability criterion

$$Ri \equiv \frac{N^2}{(\mathrm{d}u/\mathrm{d}z)^2} < Ri_{\rm crit} = \frac{1}{4} \qquad (1)$$

(see *e.g.* Chandrasekhar 1961). This is a *non-linear* condition for instability.

1.1.1. Dynamical shear instability

Along isobars, there is no restoring force, and thus, shear is unstable as soon as horizontal differential rotation is present; this is a *dynamical* instability, acting on a dynamical hence quite short time-scale and leading to a large

horizontal turbulent viscosity. It is not well constrained yet, but may have strong implications on the *vertical* transport of elements (see § 1.2.3 and 1.4; this is also discussed at length in Talon et al. 2005).

1.1.2. Secular shear instability

In the direction of entropy stratification, both the thermal and the mean molecular weight stratifications hinder the growth of the instability. However, thermal diffusion and horizontal shear act as to reduce the stabilizing effect of the stratification. We obtain the *instability* criterion

$$\left(\frac{\Gamma}{\Gamma+1}\right)N_T^2+\left(\frac{\Gamma_\mu}{\Gamma_\mu+1}\right)N_\mu^2<Ri_{\rm crit}\left(\frac{{\rm d}u}{{\rm d}z}\right)^2 \quad (2)$$

where $\Gamma = v\ell/K_T$ and $\Gamma_\mu = v\ell/K_\mu$ (Talon & Zahn 1997, see also Maeder 1995). We normally use $Ri_{\rm crit} = 1/4$, but this is open to discussion (see *e.g.* Canuto 1998) This criterion implies that for small eddies, thermal diffusivity and horizontal shear are quite efficient to reduce stabilization by the vertical stratification. In fact, there always exists an eddy that is small enough so that the instability criterion (2) will be satisfied. Turbulent diffusivity corresponds to the largest eddy satisfying (2); this is a nonlinear description, based on energy considerations.

1.2. Meridional circulation

The Eddington-Sweet meridional circulation is related to the thermal imbalance that is in general present in rotating stars (von Zeipel 1924), and that can be compensated for by a large scale advection of entropy S

$$\rho T\boldsymbol{u}\cdot\boldsymbol{\nabla}S=\boldsymbol{\nabla}\cdot(\chi\boldsymbol{\nabla}T)+\rho\varepsilon \quad (3)$$

(Vogt 1925; Eddington 1925). $\boldsymbol{u}$, the meridional circulation velocity, is calculated with the above equality (see Fig. 1). This was done in the case of solid body rotation by Sweet (1950) and yields a large scale circulation that rises at the pole and sinks at the equator. This large scale circulation advects angular momentum as well as entropy and will modify the rotation profile; hence feedback must be treated.

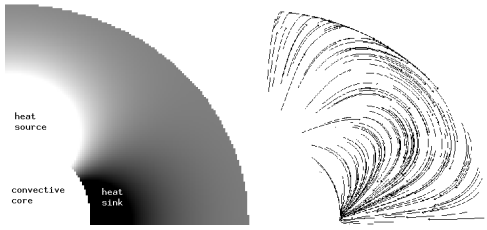

Fig. 1. The traditional approach to meridional circulation consists of calculating the thermal imbalance for a given rotation state (left, here in the case of solid body rotation with an oblateness of 10%) and evaluating the advective flux required to counter-balance this imbalance (right).

Since this is actually (at least) a 2–D effect, not much progress has been made in incorporating it into stellar evolution codes until quite recently. In a first step, models where built by treating the advection of momentum as a purely diffusive process (Endal & Sofia 1976, 1978, Pinsonneault et al. 1989, Langer 1991, these codes are still in use). A more refined description has been made by Zahn (1992); under the assumption of highly anisotropic turbulence, with the vertical turbulent viscosity ν_v being much smaller than the horizontal turbulent viscosity ν_h, the rotation state is assumed "shellular" (*i.e.* $\Omega = \Omega(P)$). In this case, the heat flux divergence of Eq. (3) can be evaluated, and used as the source term of meridional circulation.

1.2.1. Angular momentum transport

If the only transport processes present are meridional circulation and vertical turbulence, the distribution of angular momentum within the star will evolve according to an advection-diffusion equation

$$\rho\frac{{\rm d}(r^2\Omega)}{{\rm d}t}=\frac{1}{5r^2}\frac{\partial(\rho r^4\Omega u)}{\partial r}+\frac{1}{r^4}\frac{\partial\left(\rho\nu_v r^4\frac{\partial\Omega}{\partial r}\right)}{\partial r} \quad (4)$$

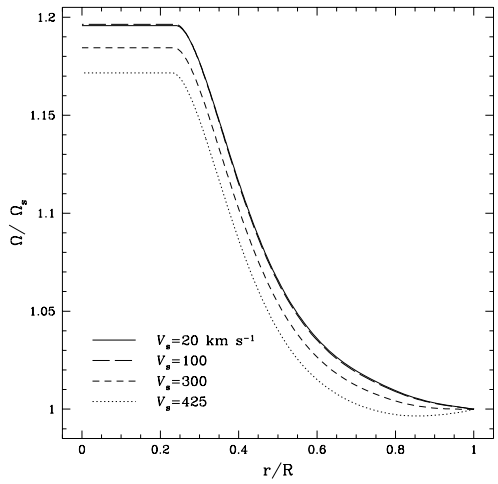

Fig. 2. Equilibrium rotation profile as given by Eq. (4) for various surface velocities in a 9 $M_\odot$ main sequence star. From Talon et al. 1997.

Note that the first term of this equation still corresponds to an advective process since, even if Ω is homogeneous on isobars, $s^2\Omega$ is not. This will not be the case for chemicals (see § 1.2.3). ν_v is a vertical turbulent viscosity, attributed to relevant rotational instabilities. Neglecting the star's evolution, this equation admits a stationary solution in which advection is counterbalanced by turbulent diffusion. In the absence of turbulence and if the star is homogeneous, circulation will simply stop, resulting in a rotation profile with a core rotating about 20% faster than the surface (Urpin et al. 1996, Talon et al. 1997, see also Fig. 2). The equilibrium profile in Θ thus depends on the nature and the vigor of rotational instabilities present in the star. However, when using realistic values for ν_v, it varies only slightly, and so, meridional circulation is in general much weaker than predicted by the simple Eddington-Sweet solution. For any rotation profile, the direction of the circulation can be deduced from the requirement of reconstructing this equilibrium solution.

If the star is not chemically homogeneous, meridional circulation will transform the vertical chemical stratification into horizontal variations of mean molecular weight that contribute to the heat flux via the equation of state. The new equilibrium requires an increase in differential rotation (compared to the homogeneous case) in order to maintain the asymptotic solution (Talon et al. 1997, Palacios et al. 2003). If the star is constrained to rotate as a solid body and does not evolve, the build up of these horizontal mean molecular weight fluctuations can lead to a circulation free state, as originally suggested by Mestel (1953). In an evolving stellar model, the required equilibrium profile also evolves. This leads to the appearance of a "re-adjustment" circulation, which is added to the asymptotic circulation. This circulation cannot be avoided, even in chemically inhomogeneous stars rotating as solid bodies.

1.2.2. Wind-driven circulation

If the star's surface is braked via a magnetic torque, as is the case of Pop I stars cooler than about 7000 K, the internal distribution of angular momentum is rapidly moved away form its equilibrium profile, with large shears developing in the outer regions. This is the regime of "wind-driven" circulation, and the model presented up to now predicts strong mixing related to such a state.

1.2.3. Chemical transport

In the case of chemical elements, the combined effect of meridional circulation and (strong) horizontal turbulence leads to (vertical) diffusion (Chaboyer & Zahn 1992, Charbonneau 1992). This is the case because horizontal turbulence continually reduces horizontal chemical inhomogeneities, impeding efficient advection. The advection + horizontal diffusion + vertical diffusion equation can then be replaced by a purely diffusive equation, with vertical turbulent transport and an effective diffusivity depending on horizontal turbulent transport D_h and advective velocity u

$$\rho\frac{\mathrm{d}c}{\mathrm{d}t} = \rho\dot{c} + \frac{1}{r^2}\frac{\partial}{\partial r}\left[r^2\rho V_{ip}c\right] +$$

$$\frac{1}{r^2}\frac{\partial}{\partial r}\left[r^2\rho\,(D_{\rm eff}+D_v)\,\frac{\partial c}{\partial r}\right] \qquad (5)$$

The effective diffusivity is $D_{\rm eff} = r^2u^2/\,(30D_h)$ (Chaboyer & Zahn 1992); $\dot{c}$ is the nuclear production/destruction rate of the species, and V_{ip} is the atomic diffusion velocity.

1.3. Some applications of rotational mixing

This theory of rotational mixing based on an advective formulation of meridional circulation and shear instabilities has been applied to a wide variety of stars. In the case of massive stars, extensive studies have been conducted by the Geneva group, with great success in explaining problems such as:

- He and N overabundances in O- and early B-type stars and in super-giants;
- the number ratio of red to blue super-giants;
- the Wolf-Rayet to O-type stars ratio.

Recent results regarding massive stars are given in Meynet (2007).

In the case of low mass stars, rotational mixing has been applied to the case of the lithium dip. In this model, the hot side of the lithium dip corresponds to stars that suffer magnetic braking; this induces strong internal differential rotation, increasing rotational mixing and thus, surface lithium depletion. Rotational mixing reproduces well the hot side of the dip (Talon & Charbonnel 1998, Palacios et al. 2003) but fails for temperatures below $T_{\rm eff} \lesssim 6700$ K.

Rotational mixing has also been applied to the study of the solar rotation profile. According to helioseismology, the solar radiative zone is rotating more or less as a solid body. In that case, complete self-consistent calculations predict that radial differential rotation remains large at the solar age. This was shown independently by two groups, using slightly different approaches to rotational mixing and three different stellar evolution codes (Pinsonneault et al. 1989, Chaboyer et al. 1995, Talon 1997).

These results on low-mass stars indicate that there must be another efficient transport process for angular momentum active when the surface convection zone appears; this would explain both the solar rotation profile and the rise of the lithium abundance on the cool side of the dip (Talon & Charbonnel 1998).

1.4. Open problems in rotational mixing

The 1–D modeling of meridional circulation is an important step in understanding and testing models of stellar evolution with rotation. However, one must not forget that it is actually an advective transport and this remains an approximation. The major limitation of the model comes from the invoked horizontal turbulent diffusion coefficient D_h. While in actual models it is linked to the source of horizontal shear (that is, some function of u) its magnitude remains quite uncertain. Furthermore, the hypothesis is that its effect will be to smooth out horizontal fluctuations. This is the case in the Earth's atmosphere albeit only up to scales that are smaller than the Rossby radius[1], which is given by $L_{\rm Rossby} = (H_P N)/(2\Omega \sin\theta)$ where θ is the latitude. With typical values for H_P and N, it is of order $L_{\rm Rossby} \simeq (50R)/(v_{\rm rot}\sin\theta)$, with $v_{\rm rot}$ in km s^{-1}. This limit will thus become relevant for stars rotating faster than about 100 km s^{-1}.

Another issue concerns the vertical transport of chemicals in the presence of strongly anisotropic turbulence. As a turbulent eddy is displaced vertically in the fluid, it looses some of its coherence by being mixed by horizontal turbulence. This effect has been demonstrated in numerical simulations (Vincent et al. 1996, Toqué et al. 2006). Talon et al. (2006) showed that such erosion is essential in the context of AmFm stars. However, such a reduction would degrade the good agreement obtained in the case of massive stars.

We are awaiting the results of 2–D (Garaud 2002) and 3–D (Talon et al. 2003) numerical simulations to improve this description.

[1] This scale is the one at which Coriolis' force becomes comparable to vertical stratification.

2. Magnetic fields

2.1. Solar spin-down

Probably the best known effect of magnetic fields is to produce solid body rotation along field lines: this is a restatement of Ferraro's theorem (1937). An obvious solution to the solar radiative zone spin-down problem is to invoke the presence of a fossil magnetic field, as described at length by Mestel & Weiss (1987). Charbonneau & MacGregor (1993, see also Barnes et al. 1999) studied this effect in a 2–D solar model, assuming a *fixed* poloidal configuration. They applied surface braking to a star originally rotating at 50 $\Omega_{\odot}$. In these simulations, as the surface is spun-down, the poloidal field is sheared; this builds up a toroidal field that will then, through the Lorentz force, oppose the shear. When latitudinal differential rotation in the convection zone is present, it may imprint itself in the interior (MacGregor & Charbonneau 1999). Agreement with helioseismic inversion require that the field be totally contained in the radiative zone.

Recent 3–D MHD numerical simulations in which the fossil poloidal field is allowed to evolve have been performed to study this mechanism in a fully consistent way, using the ASH code (Brun & Zahn 2006). In all cases studied by these authors, the fossil field is found to diffuse outwards and inexorably connects with the outer convection zone, imprinting its differential rotation to the radiative interior. Contrary to the expectation of Gough & McIntyre (1998), the meridional flow that develops between the base of the convection zone and the dipole poloidal field is not able to stop its progression. It remains to be seem whether things would change if lower (more realistic) values of the magnetic diffusivity, thermal diffusivity and viscosity were used (this is currently out of reach numerically).

2.2. Magnetic stability

Another issue that needs concern stellar astrophysicists regarding magnetic fields is that of the magnetic stability. This is well illustrated by the following quote from Braithwaite & Spruit (2004): *"Although there have been educated guesses as to what shape a field in a stable equilibrium might have, all configurations studied with the analytic methods available so far were found to be unstable on the Alfvén timescale; it has been impossible to prove stability for even a single field configuration."*

The issue of magnetic stability in rotating stars has been studied theoretically in great details by several authors, and an extensive review of these can be found in Tayler (1973) and Pitts & Tayler (1985). These linear stability study are performed using perturbations of the equations for the conservation of mass, momentum and energy and the magnetic induction equation and verifying whether a lower energy state exists. Actual calculations are time consuming, and have to be made for each magnetic configuration. The relative efficiency of these instabilities was reexamined by Spruit (1999), and he concluded that, the *pinch-type instability*, which is now more widely known as the *Tayler-Spruit instability* in the stellar community, was the first to set in.

In this instability, the toroidal field produces a poloidal field. Spruit (2002) also studied the regeneration of the toroidal field, leading to a complete dynamo. From the saturation of this cycle, he obtained an expression for magnetic stresses that act on angular momentum just like a (large) viscosity (see also Maeder & Meynet 2004, we refer the reader to the original papers for the mathematical description).

2.2.1. Applications to stars

This model has been applied by the Geneva group to a variety of stellar models. This process is highly efficient in reducing differential rotation. In the case of massive stars, rotation gradients are strongly reduced by the Tayler-Spruit instability (Maeder & Meynet 2004). Shear instabilities become much less important in this case, while meridional circulation is revived, since the rotation profile remains far from the one required by thermal equilibrium (§ 1.2). These results are discussed at length by Meynet (2007).

In the case of the Sun, the Tayler-Spruit instability also strongly reduces differential rotation. This was tested in an evolutionary model of a 1 $M_\odot$ model, in which are also included meridional circulation and shear instability (Eggenberger et al. 2005). This study confirms the capability of this process to reproduce the Sun's flat rotation profile.

2.3. Open problems in the coupling of magnetic fields and rotation

The existence of the Tayler-Spruit instability has been observed in numerical simulations (Braithwaite 2006). However, the interaction of this instability with the star's rotation implicitly assumes the regeneration of a large scale, axisymmetric poloidal field from which the toroidal field can be generated. However, the "kink" instability described here corresponds to a global $m = 1$ mode, and so generates a poloidal field with a similar angular dependence. This absence of a "closed" dynamo was observed in numerical simulations by Zahn et al. (2007). It remains to be seen if it would occur in conditions with smaller values of η and ν as expected in stellar interiors.

Another approach to the interaction of magnetic fields and rotation consists in adding the Lorentz force in the equations for meridional circulation (Mathis & Zahn 2005). This leads to a complex set of 16 coupled differential equations that has not yet been included in actual stellar evolution calculations.

3. Internal gravity waves

In astrophysics, internal gravity waves have initially been invoked as a source of mixing for elements induced by a variety of mechanisms (Press 1981, García López & Spruit 1991, Schatzman 1993, Montalbán 1994, Young et al. 2003). Ando (1986) studied the transport of momentum associated with standing gravity waves; he showed how angular momentum redistribution by these waves may increase the surface velocity to induce episodic mass-loss in Be stars (see also Lee 2006). He was the first to clearly state (in the stellar context) the fact that waves carry angular momentum from the region where they are excited to the region where they are dissipated. Goldreich & Nicholson (1989) later invoked gravity waves in order to explain the evolution of the velocity of binary stars, producing synchronization that proceeds from the surface to the core. Traveling internal gravity waves have since been invoked as an important process in the redistribution of angular momentum in single stars spun down by a magnetic torque (Schatzman 1993, Kumar & Quataert 1997, Zahn et al. 1997, Talon et al. 2002).

3.1. Excitation of internal waves

In the single star context, we are interested in waves produced by the injection of kinetic energy from a turbulent region to an adjacent stable region. Such a process is observed in numerical simulations of penetrative convection both in 2–D and 3–D (Hurlburt et al. 1986, Andersen 1994, Nordlund et al. 1996, Kiraga et al. 2000, Dintrans et al. 2005, Rogers & Glatzmeier 2005). They are excited by two different processes namely

- convective overshooting in a stable region;
- excitation by the Reynolds stresses in the convection zone itself.

Both sources contribute to the excitation. We are still awaiting reliable prescriptions for these processes since current theoretical models (García López & Spruit 1991 for overshoot and Goldreich et al. 1994 for Reynolds stresses) are not in agreement with numerical simulations which, themselves, do not quite reproduce stellar conditions properly.

3.2. Momentum transport

Waves conserve their angular momentum as long as they are not damped. The non-local nature of this transport it what makes it so efficient. In stars, the most efficient damping process is heat diffusion by photon exchange, producing an attenuation factor proportional to the thermal diffusivity, and inversely proportional to the wave's frequency and wavelength. Locally, the total angular momentum luminosity $\mathcal{L}_J(r)$ is the sum of the contribution of all

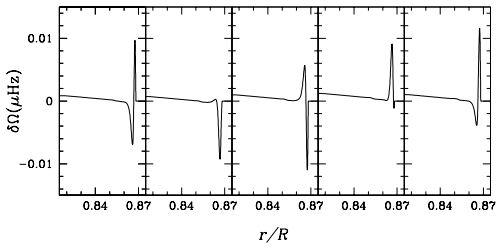

Fig. 3. Shear layer oscillation (SLO) in a 1.3 $M_\odot$ model. Successive profiles are separated by 1 year intervals. The layer's thickness depends on the magnitude of thermal dissipation and the oscillation period is a function of the total wave angular momentum luminosity.

waves. The deposition of angular momentum is then given by the radial derivative of this luminosity. The evolution of angular momentum then follows

$$\rho \frac{\mathrm{d}}{\mathrm{d}t}\left[r^2\Omega\right] = \pm\frac{3}{8\pi}\frac{1}{r^2}\frac{\partial}{\partial r}\mathcal{L}_J(r). \quad (6)$$

The "+" ("−") sign in front of the angular momentum luminosity corresponds to a wave traveling inward (outward). This term should be added to the contribution of other transport processes.

3.2.1. Wave-mean flow interaction and the SLO

We now examine the impact of IGWs on the radial distribution of angular momentum. For low frequency waves, damping is strong enough so that most waves are damped very close to the base of the convection zone. These are the waves we will examine here.

Let us assume that prograde and retrograde waves are excited with the same amplitude. In solid body rotation, these are equally dissipated when traveling inward and have no impact on the distribution of angular momentum. In the presence of differential rotation, the situation is different. If the interior is rotating faster than the convection zone, the local frequency of prograde waves diminishes, which enhances their dissipation; the corresponding retrograde waves are then dissipated further inside. This produces an increase of the local differential rotation, and creates a double-peaked shear layer. In the presence of shear turbulence, this layer oscillates (SLO, *cf.* Fig. 3 and Ringot 1998, Kumar et al. 1999). Viscosity is essential in this process and is responsible for the disappearance of the outermost peak as its slope gets steeper and the peak is slowly absorbed by the convection zone.

3.2.2. Secular effects

If the radiative zone has the same rotation rate as the convection zone, over a complete SLO cycle, the magnitude of the prograde and retrograde peaks are on average equal, and waves of azimuthal number $+m$ and $-m$ have (on average) equal amplitudes after crossing the SLO. In the presence of differential rotation however, with the inner part rotating faster than the outer part as is the case of a solar type star that is spun down by magnetic torque, the prograde peak is always larger than the retrograde peak and there is a net flux of negative angular momentum to be redistributed within the star's radiative zone. Talon et al. (2002) showed that this can spin down the interior of a star over long time-scales. Talon & Charbonnel (2005) later showed that this *asymmetric filtering* depends only on the difference of rotation rates at the base of the convection zone and at the base of the SLO ($\delta\Omega = \Omega_{\rm cz} - \Omega_{\rm SLO}$). In fact, the asymmetry remains even in the absence of a SLO.

3.3. Applications of angular momentum transport

3.3.1. The solar rotation

This description of IGWs has been applied to the solar rotation problem. Charbonnel & Talon (2005) showed that, at the age of the Sun, differential rotation indeed becomes quite small (see Fig. 4). In this simulation, low-degree waves penetrate all the way to the core and spin it down extremely efficiently, due its very small angular momentum ($\propto r^2$). Once the core has been spun down, the damping of ret-

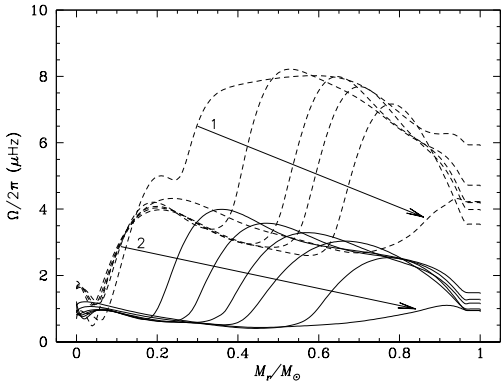

Fig. 4. Evolution of the interior rotation profile in a 1 $M_\odot$ model with meridional circulation, shear instabilities and IGWs. The initial equatorial rotation velocity is 50 km s^{-1} and surface magnetic braking is applied. Curves correspond to ages of 0.2, 0.21, 0.22, 0.23, 0.25,0.27 (dashed lines), 0.5, 0.7, 1.0, 1.5, 3.0 and 4.6 Gyr (solid lines).

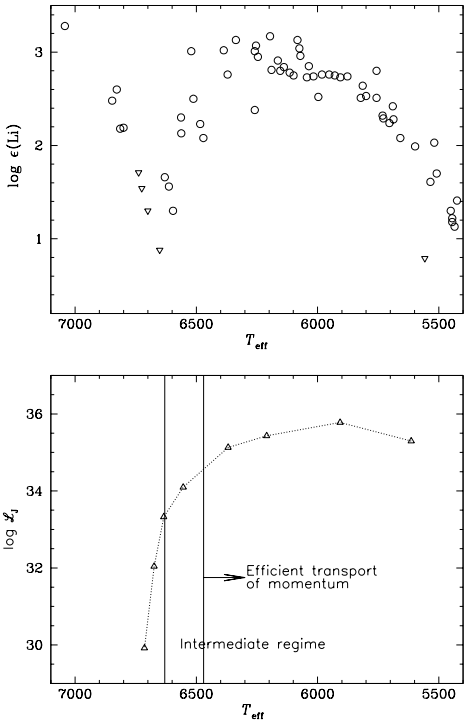

Fig. 5. (*top*) Lithium dip as observed in the Hyades. (*bottom*) Net angular momentum wave luminosity below the SLO.

rograde waves, that carry the negative angular momentum, increases locally, creating a "slowness" front that propagates in a wave-like way from the core to the surface. As further braking takes place, a second front forms and propagates outward. The differential wave filtering adjusts itself so as to compensate for the flux of angular momentum that is lost through the stellar wind. The reduced differential rotation implies a reduction in the level of lithium burning, and calculations show that it is compatible with the solar lithium. Doubt remains about reducing further lithium burning to make it compatible with recent determinations in galactic clusters of solar mass stars of the same age (see Randich, these proc.)

3.3.2. The Li dip

We mentioned (§ 1.3) that rotational mixing could explain the hot side of the Li dip but destroy too much lithium in cooler stars. If the process that is required to explain the Sun's rotation profile becomes efficient in the center of the Li dip, there reducing rotational mixing, we may obtain a model that is valid for *all* main sequence stars. Talon & Charbonnel (2003) showed that the net angular momentum luminosity corresponding to IGWs does have the proper temperature dependency (Fig. 5) and thus could well explain the cool side of the lithium dip. Complete evolutionary calculations are underway to verify this proposition.

3.4. Open problems in internal waves physics

While results obtained including internal waves in evolutionary models are quite promising, they remain crude, and several points are yet to be addressed. First of all, one should revisit the excitation of IGWs. Recent progress has been made in the description of the excitation of solar p-modes by considering better models for convection (see *e.g.* Belkacem

et al. 2006). Work is underway to adapt this description to IGWs (Belkacem et al. in prep.) Another important point is the inclusion of the Coriolis force in calculations (Talon 1997, Lee & Saio 1997, Townsend 2003, Mathis 2005, Pantillon et al. 2007). Work is underway to correctly incorporate it in descriptions of momentum transport in massive stars (Talon & Pantillon, in prep.) Finally, all calculations that are presented here correspond to horizontal averages. Implicitly, this assumes that horizontal transport is efficient in the redistribution of angular momentum along isobars. This faces the "Rossby scale problem" already mentioned in § 1.4.

References

Andersen, B.N. 1994, Solar Phys., 152, 241
Ando, H. 1986, A&A, 163, 97
Barnes, G., Charbonneau, P., & MacGregor, K.B. 1999, ApJ, 511, 466
Belkacem, K., Samadi, R., Goupil, M.J., Kupka, F., & Baudin, F. 2006, A&A, 460, 183
Braithwaite, J., & Spruit, H.C. 2004, Nature, 431, 819
Braithwaite, J. 2006, A&A, 449, 451
Brun, A.S., & Zahn J.-P. 2006, A&A, 457, 665
Canuto, V.M. 1998, ApJ, 505, L47
Chaboyer, B., Demarque, P., & Pinsonneault, M.H. 1995, ApJ, 441, 865
Chaboyer, B., & Zahn, J.-P. 1992, A&A, 253, 173
Charbonneau, P. 1992, A&A, 259, 134
Charbonneau, P., & MacGregor, K.B. 1993, ApJ, 417, 762
Charbonnel, C., & Talon, S. 2005, Science, 309, 2189
Dintrans, B., Brandenburg, A., Nordlund, Å., & Stein, R.F. 2005, A&A, 438, 365
Eddington, A.S. 1925, Obs., 48, 73
Eggenberger, P., Maeder, A., & Meynet, G. 2005, A&A, 440, L9
Endal, A.S., & Sofia, S. 1976, ApJ, 210, 184
Endal, A.S., & Sofia, S. 1978, ApJ, 220, 279
Ferraro, V.C.A. 1937, MNRAS, 97, 458
Garaud, P. 2002, MNRAS, 335, 707
García López, R.J., & Spruit, H.C. 1991, ApJ, 377, 268
Goldreich, P., & Nicholson, P.D. 1989, ApJ, 342, 1079
Gough, D. O., & McIntyre, M.E., 1998, Nature 394, 755
Hurlburt, N.E., Toomre, J., & Massaguer, J.M. 1986, ApJ, 311, 563
Kiraga, M., Różyczka, M., Stepien, K., Jahn, K., & Muthsam, H. 2000, Acta astron., 50, 93
Kumar, P., & Quataert, E.J., 1997, ApJ 475, L143
Kumar, P., Talon, S., & Zahn, J.-P. 1999, ApJ, 520, 859
Langer, N. 1991, A&A, 243, 155
Lee, U. 2006, MNRAS, 365, 677
Lee, U., & Saio, H. 1997, ApJ, 491, 839
MacGregor, K.B., & Charbonneau, P. 1999, ApJ, 519, 911
Maeder, A. 1995, A&A, 299, 84
Maeder, A., & Meynet, G. 2004, A&A, 422, 225
Mathis, S. 2005, PhD thesis, Univ. de Paris VII
Mathis, S., & Zahn, J.-P. 2005, A&A, 440, 653
Mestel, L. 1953, MNRAS, 113, 716
Mestel, L., & Weiss, N.O. 1987, MNRAS, 226, 123
Meynet, G. 2007, in Stellar Nucleosynthesis: 50 years after BBFH, Eds. C. Charbonnel, J.-P. Zahn, EAS Publ. Series, in press
Montalbán, J. 1994, A&A, 281, 421
Nordlund, Å., Stein, R.F., & Brandenburg, A. 1996, Bull. Astron. Soc. of India, 24, 261
Palacios, A., Talon, S., Charbonnel, C., & Forestini, M. 2003, A&A, 399, 603
Pinsonneault, M.H., Kawaler, S.D., Sofia, S., & Demarque, P. 1989, ApJ, 338, 424
Pitts, E., & Tayler, R.J. 1986, MNRAS, 216, 139
Press, W.H. 1981, ApJ, 245, 286
Rayleigh, L. 1880, Proc. London Math. Soc., 11, 57
Ringot, O. 1998, A&A, 335, 89
Rogers, T.M., Glatzmeier, G.A. 2005, MNRAS, 364, 1135
Schatzman, E. 1993, A&A, 279, 431
Spruit, H.C. 1999, A&A, 349, 189
Spruit, H.C. 2002, A&A, 381, 923
Sweet, P.A. 1950, MNRAS, 110, 548
Talon, S. 1997, Ph.D. Thesis, Observatoire de Paris

Talon, S. 2007, in Stellar Nucleosynthesis: 50 years after BBFH, Eds. C. Charbonnel, J.-P. Zahn, EAS Publ. Series, in press
Talon, S., & Charbonnel, C. 1998, A&A, 335, 959
Talon, S., & Charbonnel, C. 2003, A&A, 405, 1025
Talon, S., & Charbonnel, C. 2005, A&A 440, 981
Talon, S., Kumar, P., & Zahn, J.-P. 2002, ApJ, 574, L175
Talon, S., Richard, O., & Michaud, D. 2006, ApJ, 645, 634
Talon, S., Vincent, A., Michaud, G., & Richer, J. 2003, J. Comp. Phys., 184, 244
Talon, S., & Zahn, J.-P. 1997, A&A, 317, 749
Talon, S., Zahn, J.-P., Maeder, A., & Meynet G. 1997, A&A, 322, 209
Tayler, R.J. 1973, MNRAS, 161, 365
Toqué, N., Lignières, F., & Vincent, A. 2006, GAFD, 100, 85
Townsend, R.H.D. 2003, MNRAS, 340, 1020
Urpin, V.A., Shalybkov, D.A., & Spruit, H.C. 1996, A&A, 306, 455
Vincent, A., Michaud, G., & Meneguzzi, M. 1996, Phys. Fluids, 8 (5), 1312
Vogt H. 1925, Astron. Nachr., 223, 229
von Zeipel, H. 1924, MNRAS, 84, 665
Young, P.A., Knierman, K.A., Rigby, J.R., & Arnett, D. 2003, ApJ, 595, 1114
Zahn, J.-P. 1992, A&A, 265, 115
Zahn, J.-P., Mathis, S., & Brun, A.S. 2007, A&A, 474, 145
Zahn, J.-P., Talon, S., & Matias J. 1997, A&A, 322, 320